



THE UNIVERSITY  
of EDINBURGH

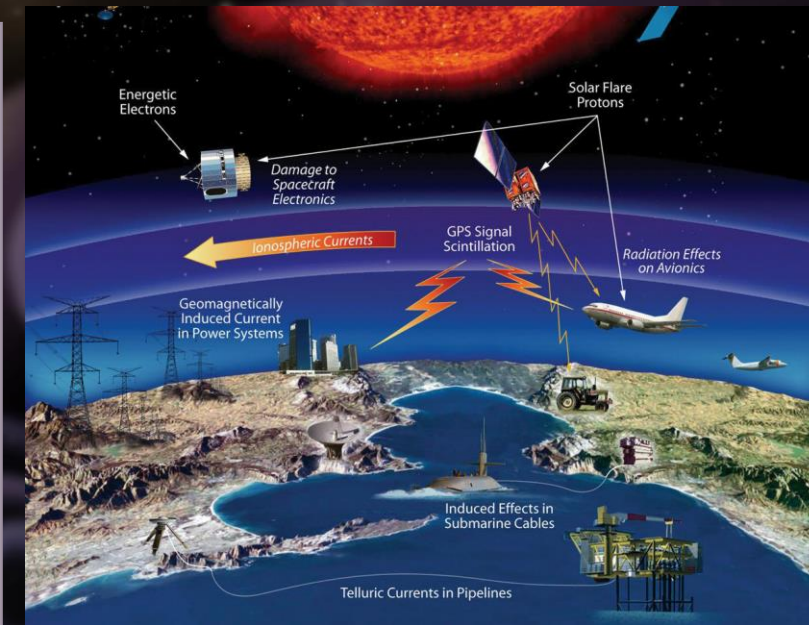
# Are magnetospheric MHD models any good for predicting magnetic field and GIC in the UK?

Ewelina Florczak<sup>1</sup>, Ciaran Beggan<sup>2</sup>,  
Kathy Whaler<sup>1</sup>

<sup>1</sup> University of Edinburgh, <sup>2</sup> British Geological Survey

## Introduction

**Space weather** events cause disturbances in the Earth's geomagnetic field. Rapid field fluctuations often result in the induction of quasi-direct currents, known as **geomagnetically induced currents (GICs)** in conductive structures on the Earth's surface. Since space weather and GICs can be damaging to various technological systems and human activity, a good forecasting capability is important in order to mitigate their impacts.



Examples of technology and infrastructure affected by space weather.  
Credit: [nasa.gov/mission\\_pages/sunearth/spaceweather/index.html](https://www.nasa.gov/mission_pages/sunearth/spaceweather/index.html)



Transformer damage in New Jersey after March 1989 geomagnetic storm.  
Credit: Public Service Electric and Gas and Peter Balma

## Aim

Accurate forecast of GIC occurrence via computational modelling can be a challenging task.

The main goal of this study is to assess the performance of currently available **MHD models** in ground magnetic field and GIC prediction in the UK.

# Experimental Method

Identifier	Model	Details
SWMF	Space Weather Modeling Framework version v20180525	high-resolution grid with 9,623,552 cells
SWMF_RCM	Space Weather Modeling Framework version v20180525, coupled to Rice Convection Model	high-resolution grid with 9,623,552 cells
GUMICS_a5	Grand Unified Magnetosphere-Ionosphere Coupling Simulation version 4-HC-20140326	adaptation level 5 grid with 350K cells
GORGON	Gorgon	large complex impedance ( $Z=10^{10}+10^{10(1+j)}$ ) to minimize ground contributions

**Table 1:** Details of the MHD models used in the analysis.

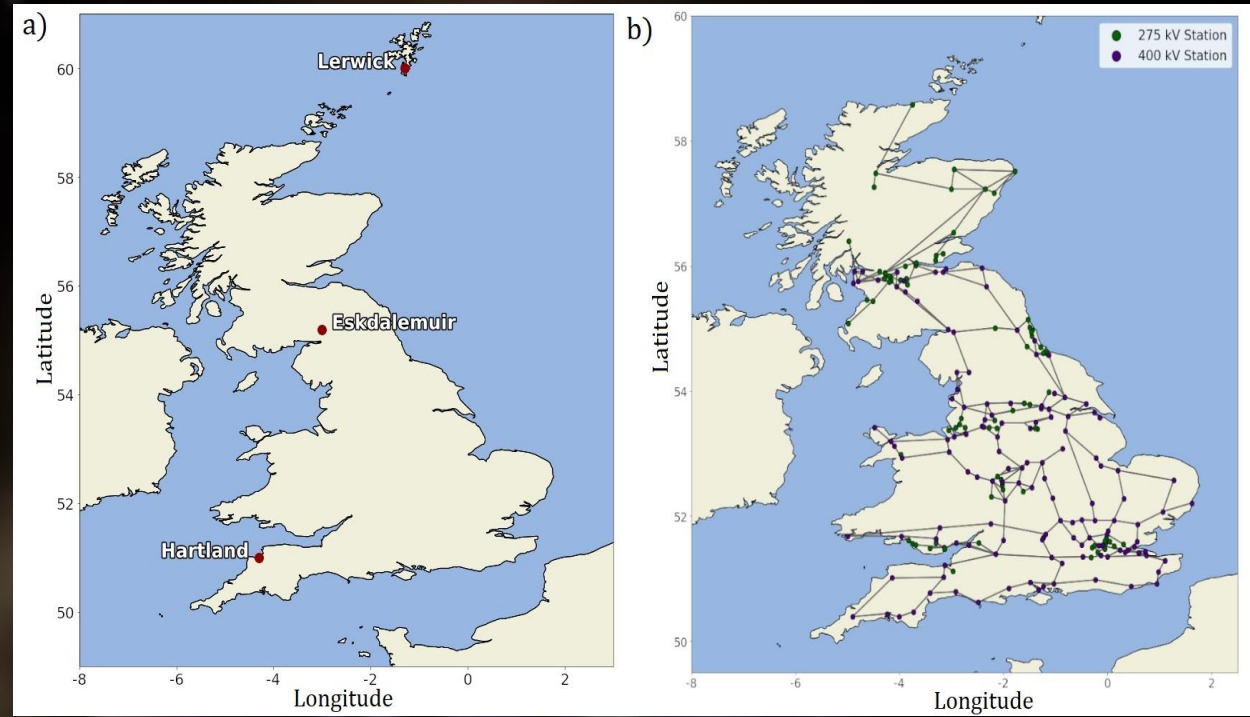


**Fig. 1:** a) Map of the UK observatories included in the study; b) Map of the UK high-voltage power network (222 substations with fixed transformer and earthing resistances).

Acquire **ground magnetic field (B-field)** measurements from 3 UK observatories (*Fig. 1a*) for 7-8 September 2017 storm.

Compare with values simulated by various **MHD models** of magnetosphere and ionosphere (*Table 1*).

Compute resulting geoelectric field (E-field), from both measured and simulated values, using **magnetotelluric transfer functions**, which relate B- and E-field components at certain location, taking into account Earth's conductivity structure.

Calculate GIC flowing through the defined network (*Fig. 1b*) using the **Lehtinen-Pirjola matrix method**:

$$[I^e] = ([\mathbf{1}] + [\mathbf{Y}^n][\mathbf{Z}^e])^{-1}[J^e]$$

where  $I^e$  is the GIC at each node,  $Y^n$  is the network admittance matrix,  $Z^e$  is the earthing impedance matrix,  $J^e$  is the voltage between nodes and  $\mathbf{1}$  represents the identity matrix.

# Initial Results

## Magnetic Field

Fig. 2 compares measured and simulated ground B-field perturbations, in nanoTeslas (nT). Left and right columns: northward and eastward components of the B-field for Hartland (HAD), Eskdalemuir (ESK) and Lerwick (LER), respectively. The black line corresponds to the measurements; coloured lines represent values simulated by each MHD model.

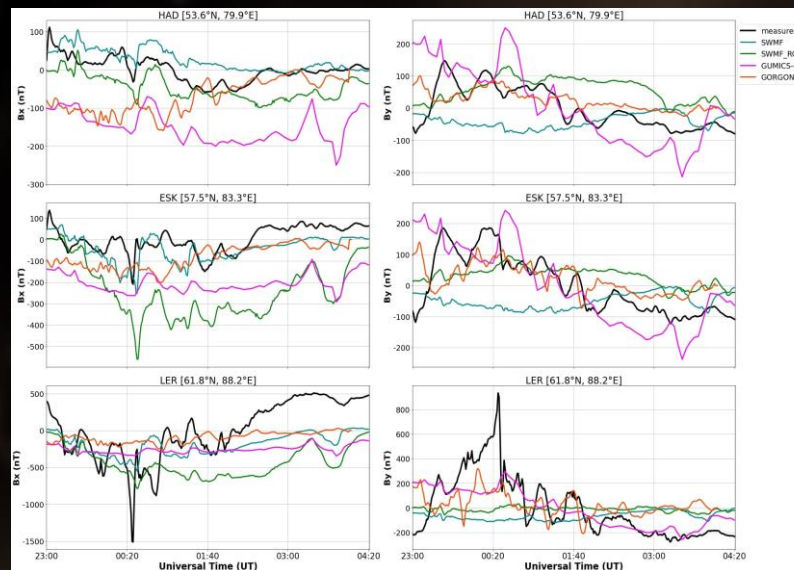


Fig. 2: Measured and modelled ground magnetic field perturbations ( $B_x$  [northward] and  $B_y$  [eastward] components).

## Goelectic Field

Fig. 3 shows the resulting northward and eastward E-field values, in millivolts per kilometer (mV/km). Layout and colours as for Fig. 2.

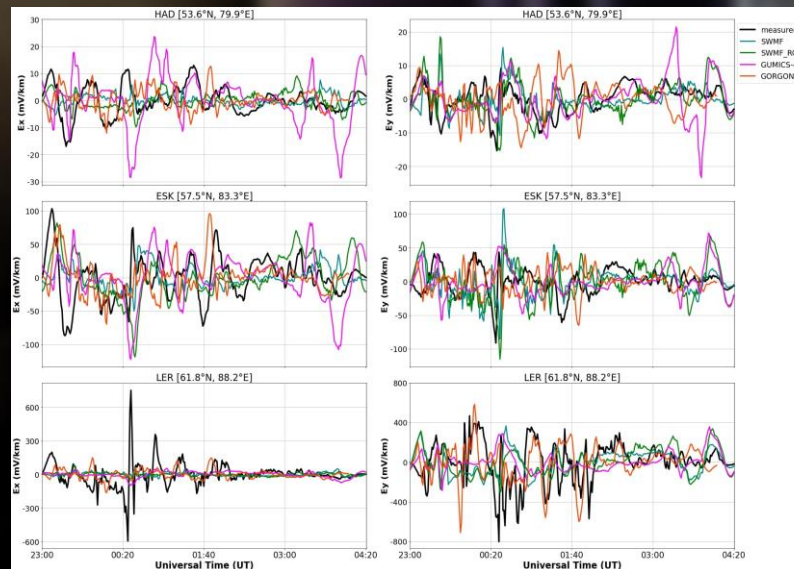


Fig. 3: Calculated geoelectric field ( $E_x$  [northward] and  $E_y$  [eastward] directions), based on measured and modelled B-field values.

## GIC

GICs calculated with a uniform geoelectric field of 1 V/km in northward and eastward orientations show that nodes close to the coastlines are affected the most (Fig. 4). For those 4 selected substations, GICs were calculated based on the extrapolated measured and modelled values obtained in previous steps (Fig. 5).

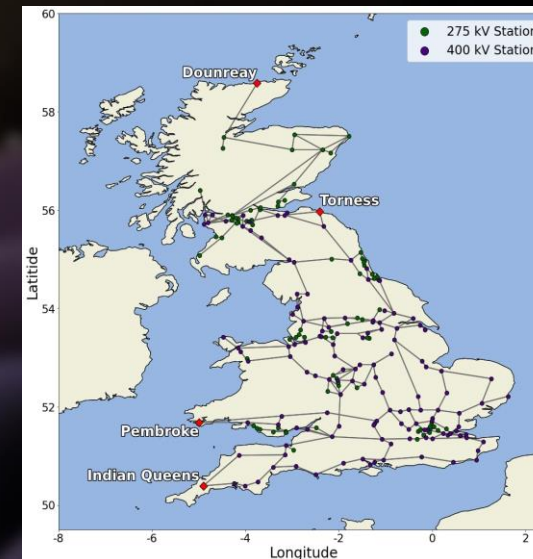


Fig. 4: Map of the UK high-voltage network with the most affected nodes indicated.

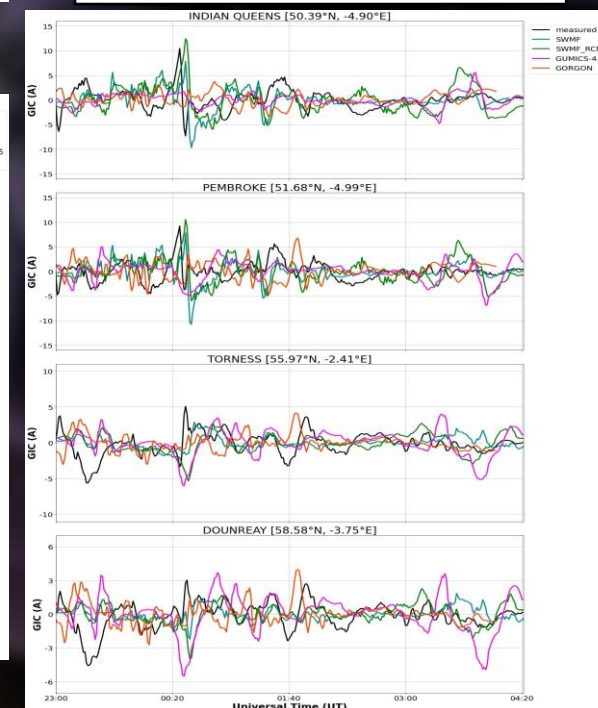


Fig. 5: Resulting GICs at each substation as a time series.

# Concluding Remarks

## Error Analysis: B-field & E-field

Modelled values of the B-field components show differences in both amplitude and temporal variability compared to the corresponding measurements.

Results shown on Fig. 6 indicate the accuracy of ground magnetic field forecast decreases with increasing latitude.

The eastward component ( $B_y$ ) tends to be predicted more accurately than the northward component ( $B_x$ ).

SWMF forecasts  $B_x$  best, whereas Gorgon forecasts  $B_y$  best.

A similar pattern was found in regards to the error analysis for the E-field results.

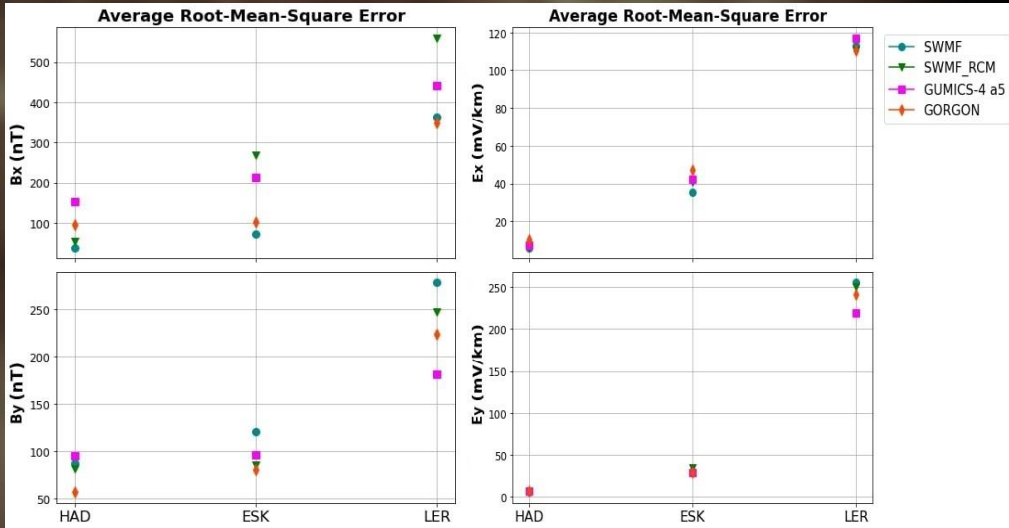


Fig. 6: Average RMSE computed for B-field (left) and E-field (right), and all observatories, arranged in order of increasing latitude, from left to right.

## Error Analysis: GIC

The error analysis (Fig. 7) suggests that GICs computed from modelled values are in closer agreement with GICs computed from measurements for nodes at higher latitudes, where the SWMF performs the best. The GICs computed for substations at lower latitudes show larger values of error. In this case, the GUMICS-4 tends to be the most accurate, despite its rather average performance in B-field forecast.

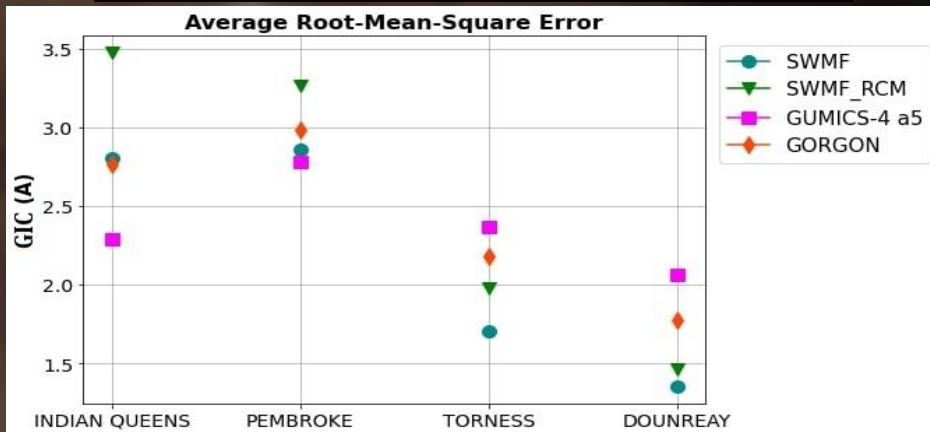


Fig. 7: Average RMSE calculated for all 4 substations.

## Future Plans

Since the accuracy of the simulation of ground B-fields by MHD models included in this study is rather unsatisfactory, attempts to improve their prediction ability will be considered.

Applying a method, commonly used in climate modelling, known as **downscaling** may potentially enhance the forecast accuracy by introducing smaller scale local variations in global variables simulated by each model.